

RSC Advances



This is an *Accepted Manuscript*, which has been through the Royal Society of Chemistry peer review process and has been accepted for publication.

Accepted Manuscripts are published online shortly after acceptance, before technical editing, formatting and proof reading. Using this free service, authors can make their results available to the community, in citable form, before we publish the edited article. This *Accepted Manuscript* will be replaced by the edited, formatted and paginated article as soon as this is available.

You can find more information about *Accepted Manuscripts* in the [Information for Authors](#).

Please note that technical editing may introduce minor changes to the text and/or graphics, which may alter content. The journal's standard [Terms & Conditions](#) and the [Ethical guidelines](#) still apply. In no event shall the Royal Society of Chemistry be held responsible for any errors or omissions in this *Accepted Manuscript* or any consequences arising from the use of any information it contains.

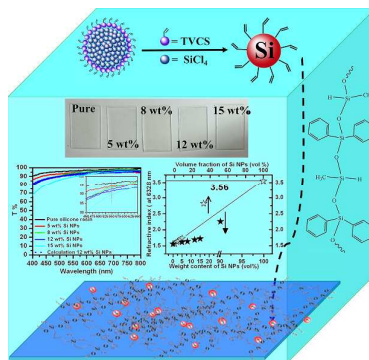
Effective increase in refractive index of novel transparent silicone hybrid films by introduction of functionalized silicon nanoparticles

Guoyan Zhang,^{+a,b} Mei Chen,^{+a} Jibin Zhang,^b Baofeng He,^{*a} Huai Yang^{*a} and Bai Yang^{*b}

Received (in XXX, XXX) Xth XXXXXXXXXX 20XX, Accepted Xth XXXXXXXXXX 20XX

DOI: 10.1039/b000000x

Refractive index of novel transparent silicone hybrid films can be effectively enhanced by introduction of functionalized silicon nanoparticles via a facile strategy.





Journal Name

ARTICLE

Effective increase in refractive index of novel transparent silicone hybrid films by introduction of functionalized silicon nanoparticles

Guoyan Zhang,^{†a,b} Mei Chen,^{‡a} Jibin Zhang,^b Baofeng He,^{*a} Huai Yang^{*a} and Bai Yang^{*b}Received 00th January 20xx,
Accepted 00th January 20xx

DOI: 10.1039/x0xx00000x

www.rsc.org/

Transparent silicone-based polymers have potential and practical applications in many optical devices, however, the chemical structure restricts their refractive indices in a lower value which cannot meet the demands of the devices. Here, we present an effective and friendly method to increase the refractive index of silicone hybrid films by combining a novel phenyl-oligosiloxane monomers and vinyl-Si NPs. The refractive index of the films (~0.1 mm, at 632.8 nm) effectively increased from 1.563 to 1.727 by varying the contents of Si NPs and showed excellent optical transparency (~0.1 mm, > 90% at 550 nm). What's more, all of the films held a sufficient pencil hardness (2H~3H). This strategy is reported for the first time for facile synthesis and effective increase the refractive index of transparent silicone hybrid films by introduction of functionalized Si NPs. Such silicone films can be potentially used to fabricate multifunctional devices or optical materials with tunable refractive indices.

Introduction

Silicone-based polymers with high transmittance and excellent thermal resistance have been widely applied to various devices such as microlenses, liquid-crystal displays, optical coatings, optoelectronic packages.¹⁻⁶ With the increasing demands for high performance in these applications, enhanced refractive index materials are strongly desired. Although the silicone-based polymers are well suited for these applications, the chemical structure restrict their refractive indices in a low value of 1.56 which cannot meet the demands of the devices.⁶⁻⁸ Scientists have long-standing enthusiasm in the development of increasing the refractive index by introducing highly polarizable heteroatoms or rigid aromatic moieties into the side chain of the silicone polymers, but the refractive index of these novel silicone polymers remain stay in a relative small adjustable range of 1.54-1.60 which are still not meeting the rapid development of the technologies.⁹⁻¹¹

Besides the strategy of incorporating high molar refractions organic groups, embedding high refractive index inorganic nanoparticles (NPs) (PbS,^{12,13} ZnS,¹⁴⁻¹⁷ TiO₂,¹⁸⁻²¹ ZrO₂,²²⁻²³ GNPs (graphene nanoparticles),²⁴ Si NPs,^{25,26}) into the organic matrices has been confirmed another effective method of increasing refractive index. For instance, the introduction of PbS particles in an organic matrix can increase the refractive

index to value of 2.5-3.0 at 632.8 nm, rendering the nanocomposite suitable material for optical applications such as the manufacture of improved efficiency solar cells.^{12,27-29} One important issue involved in the idea of introducing nanoparticles into the silicone matrices is how to maintain the transmittance of the silicone, in other words, how to avoid the light scattering and phase separation caused by the nanoparticles. Plenty of research works have been reported that particles with a small size below their Bohr diameter will minimize the scattering and using small organic molecule modified the small particles can improve their distribution and then avoid aggregation.^{12,30-31} It should be noted that, the small organic molecule usually have a lower refractive index compared with the neat nanoparticles which will directly influence the refractive index of the final modified-nanoparticles.^{14,32-34} Thus, it is still a technological challenge topic of how to utilize an effective method to incorporate nanoparticles into silicone matrices for transparent high refractive index optical materials.

In view of the above mentioned issues, and using the previous strategies as inspiration, we present an effective and friendly method to synthesize transparent silicone hybrid films with tunable and enhanced refractive index at different contents of functionalized silicon nanoparticles (Si NPs). The silicone hybrid films (~0.1 mm) with different contents of Si NPs (5 wt%-15 wt%) have enhanced tunable refractive index (1.621-1.727 at 632.8 nm) compared with neat silicone resin (1.563). What is more, these films maintained the high transmittance in the visible range (~0.1 mm, > 90% at 550 nm), and a sufficient pencil hardness (~3 H). This strategy is reported for the first time for facile synthesis and effective increase the refractive index of transparent silicone hybrid films via the introduction of functionalized Si NPs.

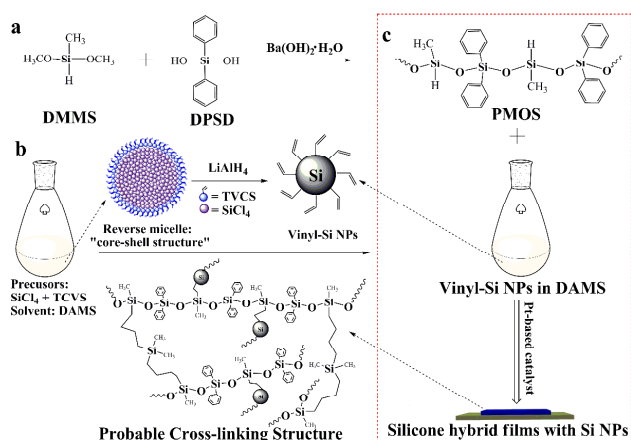
^aDepartment of Materials Science and Engineering, College of Engineering, Peking University, Beijing 100871, P. R. China.
E-mail: yanghuai@coe.pku.edu.cn.

^bState Key Laboratory of Supramolecular Structure and Materials, College of Chemistry, Jilin University, Changchun, 130012, P. R. China.
E-mail: byangchem@jlu.edu.cn.

[†] Electronic Supplementary Information (ESI) available. See DOI: 10.1039/x0xx00000x

[‡] These authors contributed equally to this work.

Results and discussion



Scheme 1 Schematic of a: synthesis of novel phenyl-oligosiloxane (PMOS) by sol-gel condensation; b: preparation of vinyl-Si NPs in diallyldimethylsilane (DAMS); c: fabrication of silicone hybrid films by a hydrosilylation reaction of PMOS and vinyl-Si NPs (in DAMS).

As illustrated in Scheme 1, a novel phenyl-oligosiloxane (PMOS) was firstly synthesized as a co-monomer of the silicone hybrid films by a sol-gel condensation process (Scheme 1a). Si NPs are selected as the inorganic components due to the precursors (TCVS: trichlorovinylsilane and SiCl4) are easily dissolved in the silane-based solvent (e.g. DAMS: diallyldimethylsilane) as well as their ultrahigh refractive index of 3.91 at 620 nm which are the most competitive candidates to improve the refractive index.³¹ The Si NPs with a vinyl-group were *in-situ* fabricated in DAMS without adding any other small organic molecule (Scheme 1b). In particular, TCVS is used as both the surfactant and the precursors, which may form a reverse micelle similar with a "core_(SiCl4)-shell_(TCVS) structure" in DAMS. And then the Si NPs with vinyl groups (named vinyl-Si NPs) covering the surface can be obtained after treating with LiAlH4. Finally, the vinyl-Si NPs, along with the DAMS, will have a hydrosilylation reaction with PMOS resulting in the silicone hybrid films after adding a Pt-based catalyst (Scheme 1c).

The molecular structure of PMOS was checked by FT-IR, ²⁹Si-NMR (Fig.1) and ¹H-NMR (Fig.S1). The spectra of pristine DMMS and DPSD were also collected as shown in Fig.1a. It can be obviously found that silanols (peak around 3214 cm⁻¹, Si-OH) on DPSD and methoxy groups (peak around 2843 cm⁻¹, Si-OCH₃) as well as the methyl groups on methoxy groups (peak at 2939 cm⁻¹, C-H₃) from DMMS were no longer presented on the FTIR spectrum of PMOS, while it appeared a new strong and broad peaks around 1084 cm⁻¹ which can be assigned to the new siloxane network (Si-O-Si).⁶ These results indicate that the condensation reaction was fully completed and had formed a siloxane network. More details can be observed that the stretching vibration of Si-H (peak at 2152 cm⁻¹, Si-H) and the Si-C (peaks at 1450 cm⁻¹, 1265 cm⁻¹, 723 cm⁻¹, Si-C) of DMMS and the stretching vibration of phenyl (peaks at 1596

cm⁻¹, 1123 cm⁻¹, Si-Phenyl) of DPSD were remained after the sol-gel reaction, which can also be proved by the ¹H-NMR spectrum (Fig.S1).³⁵ It should be noted that, there are no peaks signal (around 450 cm⁻¹) detected on PMOS, which mean that the back-bone structure of Si-O-Si on PMOS not a cyclic siloxane species but a linear structure.⁶ The ²⁹Si-NMR spectrum of PMOS presented the highly condensed Si species, which further confirmed the formation of siloxane network (Fig.1b).^{36,37} Based on the ²⁹Si-NMR measurements, the degree of condensation (DOC) for the siloxane network was calculated by the following equation:³⁸

Both of DPSD and DMMS are dimeric species that are denoted as Dⁿ and Dⁿ, respectively, where the superscript "n" represents the number of siloxanes bound on a Si atom. The calculated DOC value for PMOS was 86.3%, indicating the siloxane network well-formed. Note that, there are no D⁰ and D⁰ species, confirming there are no unreacted species of DMMS and DPSD which is consistent with the previous FT-IR results.

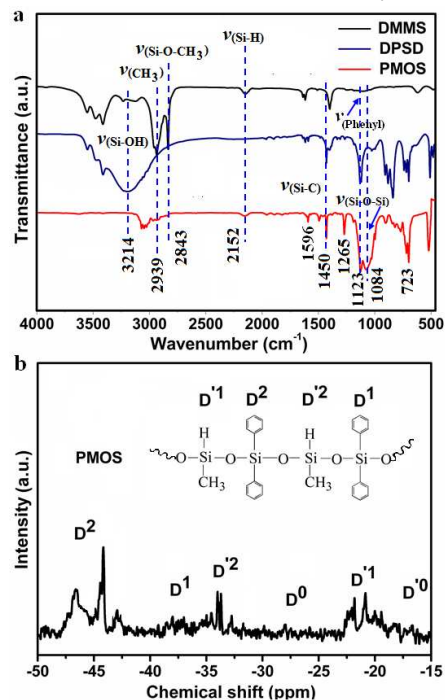


Fig.1 a: FT-IR spectra of the prepared PMOS and precursors of DMMS and DPSD; b: ²⁹Si-NMR spectrum of the prepared PMOS using chloroform-*d* as solvent.

Fig.2a presents the TEM image of the as-prepared Si NPs, appearing as spherical particles with an average size of 6 nm and having a good dispersion. High-resolved TEM (HRTEM) image (inset in Fig.2a) demonstrates the excellent crystalline structure of the as-prepared Si NPs by a clear lattice with a spacing of 0.212, which is consistent with the (220) plane of cubic crystalline Si.^{39,40} As we illustrated in Scheme 1b, the precursors (TCVS and SiCl4) of the Si NPs may form a "core_(SiCl4)-shell_(TCVS) structure" reverse micelle in DAMS, which implied

that the prepared Si NPs will be covered with the vinyl groups via the Si-C bonds. To verify this assumption, the FT-IR (Fig.2b) and $^1\text{H-NMR}$ (Fig.2c) were used to measure the surface chemistry of the as-prepared Si NPs. It can be seen that three distinct bands were shown in FT-IR (Fig.2b): the peaks around 2963 cm^{-1} are the C-H₂ stretch; the peak at 1617 cm^{-1} indicates C=C stretch due to the vinyl groups on the surface and the peak at 1271 cm^{-1} is typical for Si-C stretch.^{41,42} Moreover, the Si-Cl peak at 527 cm^{-1} is not detected, which means there are no residual precursors.⁴³ These peaks provide evidence of the as-prepared particles covered with the vinyl groups via covalent bonds. In addition, the signals at 5.91 ppm (singlet) and 4.94-5.12 ppm (doublet) appeared in $^1\text{H-NMR}$ (Fig.2c) are typical for alkene groups, which are further confirmed the as-prepared Si NPs have vinyl groups on their surface.^{40,44}

Fig.2 a:TEM and HRTEM (inset) micrographs of the synthesized Si NPs; b: FT-IR spectrum of the prepared Si NPs; c: $^1\text{H-NMR}$ spectrum of the Si NPs using chloroform-*d* as solvent.

The silicone hybrid films with varying composition from 5-15 wt% Si NPs (Fig.3a) were prepared by controlling ratios of vinyl_(DAMS+vinyl-SiNPs) and hydride_(PMOS) at 1.2:1 to ensure a complete polyreaction. The FT-IR spectra (Fig.S2) of silicone hybrid films show that the Si-CH=CH₂ at 1617 cm^{-1} and the Si-H bond at 2512 cm^{-1} are disappeared, while the Si-O-Si bond and the Si-C are still unchanged, indicating the cross-linking reaction has fully completed and the backbone of the films are consist of Si-O-Si bond (Scheme 1c). Thermal decomposition results (Fig. S3 and Table S1) show that the silicone hybrid films have similar initial decomposition temperatures compared with the neat silicone resin. The hardness of the films (Table S1) increased with an increase in Si NPs content, indicating that the Si NPs can improve the surface hardness of the films to some extent. The improved surface hardness is mainly attributed to the Si-O-Si bond, the cross-linking structures and the Si NPs.

The optical transparency of the silicone hybrid films ($\sim 0.1\text{ mm}$) on glass substrate was interrogated using UV-vis transmittance spectroscopy (Fig.3b). All of the films maintained the good transmittance in the visible range (400 – 800 nm) and the transmittance is above 89% at 550 nm (See the inset spectra), regardless of the composition of the films (See Table S1). From the inset spectra we could find that the transparency of the silicone hybrid films has a slightly decreased compared with the pure silicone resin. Generally, the large inorganic domain size and refractive index mismatch between the inorganic phase and the matrix are believed to be responsible for the decline in transparency.³⁰ In our research, the silicone hybrid films with 12 wt% Si NPs was selected as an example to explain the decline in transparency based the Rayleighs law:³¹

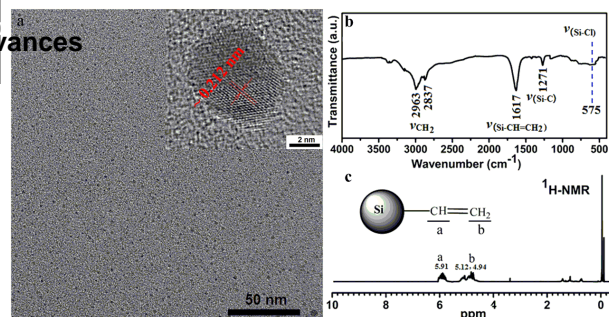


Fig. 2 with intensity I of the transmitted and I_0 of the incident light, radius r of the spherical particles, refractive index n_p of the particles and refractive index n_m of the matrix. λ is the wavelength of the light, ϕ_p the volume fraction of the particles and x the optical path length. It can be seen that the calculated result (blue dash line) is agreed well with the measured result (blue line). This result implies that the Si NPs are small enough ($\sim 6\text{ nm}$) to avoid the light scattering (Fig.3b). Note that, there is still existing a small deviation in the results as shown in the inset spectra in Fig.3b, which can be mainly assigned to the difference of the refractive indices ($n_p - n_m$) between the silicone matrix and the Si NPs.

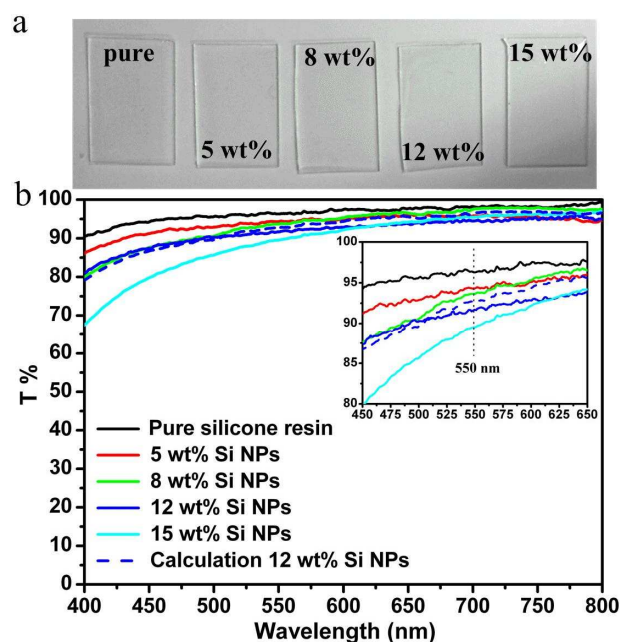


Fig.3 a: Photographs of the obtained novel silicone hybrid films on glass substrates with different weight contents of Si NPs; b: optical transmission spectra of these films. The inset shows the scale-up transmission spectra.

A homogenous dispersion of the inorganic filler on the nanoscale without any aggregation is very important for the transparent thin films, especially when it comes to structuring. The dispersion and the phase images of Si NPs in the silicone hybrid films were observed using TEM (Fig. 4a) and AFM (Fig.

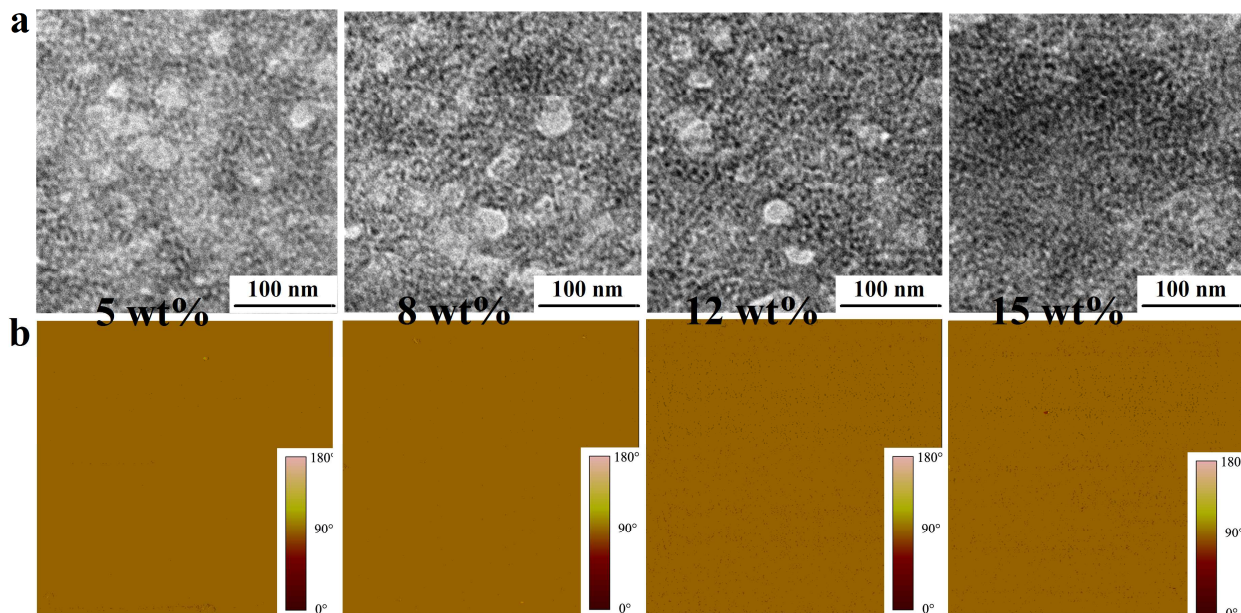


Fig. 4 TEM images (a) and AFM phase images (b) of the prepared silicone hybrid films with different weight content of Si NPs.

4b), respectively. It can be clearly seen that the Si NPs with a same diameter compared with that of Si NPs before polymerization, are homogeneously mixed within the silicone matrix without any agglomeration even at a high loading (15 wt%). The phase images of the hybrid films (Fig. 4b) show two regions (dark: Si NPs domain and bright: silicone domain) and no macro-phase separation was observed, indicating that the Si NPs are uniformly dispersed in the silicone matrix.

A prism coupling device was used to measure the refractive indices of the silicone hybrid films at 632.8 nm. Fig. 5 shows the dependence of refractive indices of silicone hybrid films versus the weight contents of Si NPs (solid pentagram) and the volume fractions of pure Si NPs (hollow pentagram). It can be seen that the refractive index has increased effectively from 1.563 to 1.727 with an increasing weight content of Si NPs from 0 to 15 wt% (Table S1). The variations of the Si NPs in the silicone matrices of the films should be accounted for the increasing refractive indices. Thus, the refractive index of the Si NPs in the silicone matrices was calculated assuming that the organic and inorganic phase have a contribution to the refractive index of the hybrid films proportional to their volume fraction:^{12,31}

$$n_{\text{SiNPs}} = \frac{n_{\text{film}} - \phi_{\text{silicone}} n_{\text{silicone}}}{1 - \phi_{\text{silicone}}}$$

$$\phi_{\text{silicone}} = \frac{w_{\text{silicone}} \rho_{\text{SiNPs}}}{w_{\text{silicone}} \rho_{\text{SiNPs}} + (1 - w_{\text{silicone}}) \rho_{\text{silicone}}}$$

Where n_{film} , n_{SiNPs} and n_{silicone} are the refractive indices of the film, the Si NPs and the silicone component; ϕ_{silicone} and ϕ_{SiNPs} are the volume fractions in the films of silicone and Si NPs; w_{silicone} is the weight fraction in the films of silicone; ρ_{SiNPs} and ρ_{silicone} are the densities of Si NPs and silicone. The value of pure Si NPs reaches 3.56 (at 632.8 nm, bigger hollow pentagram shown in Fig. 5) by regression analysis for an extrapolation to 100 vol% Si NPs. The refractive index of Si NPs in this system is smaller but close to the value of crystalline Si (3.91 at 620 nm) within experimental error, indicating our strategy avoided the loss in refractive index of neat Si NPs caused by extra small organic molecule.

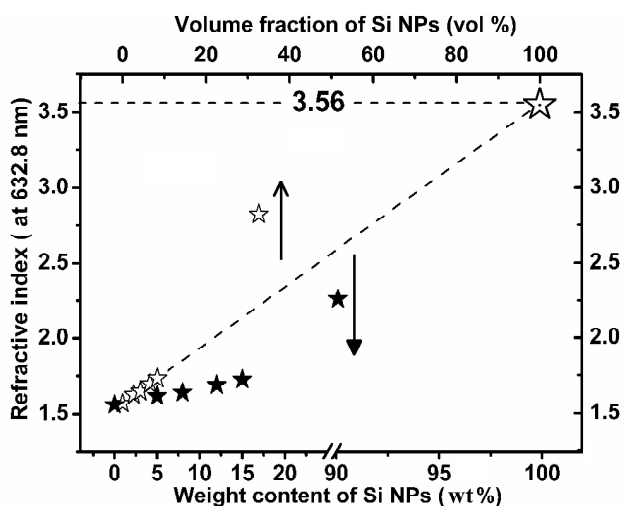


Fig.5 Refractive indices of the silicone hybrid films with different weight content (solid pentagram) and volume fractions (hollow pentagram) of Si NPs. The bigger hollow pentagram is a regression analysis for an extrapolation to 100 vol% Si NPs based the volume fractions.

Generally, the small particles with a quantum size usually have a quantum size effects which will influence the optical constants of the materials, such as the refractive index.¹² The Bohr diameter (D_b) of Si NPs was calculated about 4 nm based the following expressing:⁴⁵

$$D_b = \frac{2\pi\epsilon_0\epsilon\hbar^2}{m^*e^2}$$

where ϵ_0 and ϵ are the vacuum permittivity and the optical dielectric constant of the medium, respectively (for Si $\epsilon = 11.9$); \hbar is Planck's constant; e is the electron charge, m^* is the average effective mass of Si. The size of Si NPs in this research is about 6 nm which is close to their Bohr diameter. Therefore, the quantum size effects of Si NPs in this system are not evident on their refractive indices.

Conclusions

In summary, we have provided an effective strategy for increasing the refractive index of novel transparent silicone film by introducing functionalized Si NPs. The refractive index of the film increased from 1.563 to 1.727 by varying the contents of Si NPs and all of them showed excellent optical transparency. We confirmed that the silicone hybrid films exhibit a high decomposition temperature and a sufficient pencil hardness. Such silicone films can be potentially used to fabricate multifunctional devices or optical materials with tunable refractive indices.

Experimental

Materials

All of chemicals were used as received unless otherwise stated. Dry solvents were obtained after passing through a solvent purification system with a water content below 10 ppm. Dimethoxy(methyl)silane (DMMS, 98%, TCI), diphenylsilanediol (DPSD, 98%, TCI), $\text{Ba}(\text{OH})_2 \cdot \text{H}_2\text{O}$ (BH, Sigma-Aldrich), anhydrous toluene (TCI), diallyldimethylsilane (98%, DAMS, TCI), trichlorovinylsilane (TCVS, 98%, TCI), SiCl_4 (98%, TCI), Lithium Aluminum Hydride (10% in Tetrahydrofuran, ca. 2.5mol/L, TCI), platinum(0)-1,3-divinyl-1,1,3,3-tetramethylidisiloxane complex solution (Sigma-Aldrich), dry methanol (TCI).

Preparation of phenyl-oligosiloxane (PMOS) by a sol-gel condensation

DMMS and DPSD with an optimized molar ratio of 1:1.3 were mixed into anhydrous toluene in a flask and placed it into an oil-bath at 80 °C. Then BH was added into the solution as a catalyst (0.1 mol% of the total silane precursors) to promote the direct condensation reaction between the methoxy radical of DMMS and the diol radical of DPSD to form the siloxane bonds of oligosiloxane. The mixture was kept at 80 °C for 4 h and then cooled it down to room temperature. The byproduct methanol was removed by a rotary evaporator. BH was removed by using a 0.45 μm pore-sized Teflon filter. The residual condense liquids were named as phenyl-oligosiloxane (PMOS).

Preparation of Silicon nanoparticles with vinyl group (vinyl-Si NPs)

The reactions were performed in a nitrogen-filled glove box with oxygen and water content below 10 ppm. 0.1 mL SiCl_4 and 0.15 mL TCVS were mixed in 30 mL DAMS, followed by stirring for several minutes till forming a homogeneous transparent solution. Subsequently, 0.2 mL LiAlH_4 (reducing agent) was added to the mixture and stirred for at least 30 min. Then, 30 mL dry methanol was used to oxidize the excess LiAlH_4 followed by stirring another 30 min at least. The excess dry methanol was evaporated under reduced pressure. Finally, we obtained the solutions of Si NPs in DAMS with concentration of 2 mg/mL. For further structure characterization, the powder of Si NPs can be obtained by evaporation of the solvent at 35 °C under reduced pressure.

Preparation of silicone hybrid films with different contents of Si NPs

The synthesized monomer PMOS, as a cross-linker, was mixed with the DAMS solutions with different concentration of Si NPs (0-15 wt%: the solid Si NPs in DAMS) in a optimized molar ratio of 1.2:1 $\text{vinyl}_{(\text{DAMS}+\text{vinyl-SiNPs})} : \text{hydride}_{(\text{PMOS})}$ and a platinum(0)-1,3-divinyl-1,1,3,3-tetramethylidisiloxane complex solution (about 20 ppm) was added. Then, the mixture was dipped or spin-coated on the normal glass substrates (micro-slide) and the silicone hybrid films can be obtained by curing at 150 °C in air atmosphere for 4h. Note that, we named the films without Si NPs as neat or pristine silicone materials.

Characterization

^1H -NMR and ^{29}Si -NMR spectra were recorded with a Bruker AV600 MHz (Bruker, Germany) instrument at ambient temperature using chloroform-d as solvent. TEM and HRTEM samples, dropped on a copper grid covered with carbon film and the solvent evaporated at room temperature, were carried out using a JEM 2010 microscope. FT-IR spectra were obtained on a BrukerVector-22 FT-IR spectrophotometer using a KBr pellet over a range of 4000-400 cm^{-1} . Atomic force microscopy (AFM) analysis of the silicone hybrid films was performed in the tapping mode with a Nanoscope IIIa scanning probe microscope from Digital Instruments under ambient conditions. The optical transmittance of the films was tested on a Unico UV-4802 UV/vis spectrophotometer in a wavelength range of 300 to 800 nm. Thermogravimetric analysis (TGA) of the films was performed on a Perkin-Elmer TGA7 at a heating rate of 10 $^{\circ}\text{C}$ /min under nitrogen flow from 25-1000 $^{\circ}\text{C}$. A prism couple (Metricron, 2010) was used to measure the refractive index of the films at 632.8 nm.

Acknowledgements

The authors appreciate the Sino-American Cooperative Project of Chinese Ministry of Science and Technology under Grant (2013DFB50340) and the financial support of the National Natural Science Foundation of China (No.51302006 , 91123031, 21221063 and 50973039).

Notes and references

- W. Zhang, H. Zappe and A. Seifert, *Light Sci. Appl.*, 2014, **3**, e145.
- B. J. Scott, G. Wirnsberger and G. D. Stucky, *Chem. Mater.*, 2001, **13**, 3140-3150.
- C. Jiwon, G. K. Seung and M. L. Richard, *Macromolecules*, 2004, **37**, 99-109.
- S. Takei, K. Mochiduki, N. Kubo and Y. Yokoyama, *Appl. Phys. Lett.*, 2012, **100**, 263108.
- J. S. Wang, C. C. Tsai, J. S. Liou, W. C. Cheng, S. Y. Huang, G. H. Chang and W. H. Cheng, *Microelectron. Reliab.*, 2012, **52**, 813-817.
- J. S. Kim, S. C. Yang and B. S. Bae, *Chem. Mater.*, 2010, **22**, 3549-3555.
- J. Wang, M. L. Du, C. S. Xu, H. Zhu and Y. Q. Fu, *J. Macromol. Sci., Part B: Phys.*, 2012, **51**, 2462-2472.
- M. Zhan, Y. K. Feng, Y. Li, G. Li, Y. L. Wang, Y. Han, X. J. Sun and X. H. Tan, *J. Macromol. Sci., Part A: Pure Appl. Chem.*, 2014, **51**, 653-658.
- H. T. Cai, L. P. Zhang, Y. Xiong, Q. L. Qu and H. D. Tang, *J. Inorg. Organomet. Polym. Mater.*, 2014, **24**, 780-785.
- C. Y. Luo, J. D. Zuo, Y. C. Yuan, X. C. Lin, F. Lin and J. Q. Zhao, *Opt. Mater. Express*, 2015, **5**, 462-468.
- D. W. Mosley, G. Khanari an, D. M. Conner, D. L. Thorsen, T. L. Zhang and M. Wills, *J. Appl. Polym. Sci.*, 2014, **131**, 39824.
- T. Kyprianidou-Leodidou, W. Caseri and U. W. Suter, *J. Phys. Chem.*, 1994, **98**, 8992-8997.
- C. L. Lü, C. Guan, Y. F. Liu, Y. R. Cheng and B. Yang, *Chem. Mater.*, 2005, **17**, 2448-2454.
- C. L. Lü, Y. R. Cheng, Y. F. Liu, F. Liu and B. Yang, *Adv. Mater.*, 2006, **18**, 1188-1192.
- C. Guan, C. L. Lü, Y. R. Cheng, S. Y. Song and B. Yang, *J. Mater. Chem.*, 2009, **19**, 617-621.
- G. Y. Zhang, J. B. Zhang and B. Yang, *Polym. Chem.*, 2013, **4**, 3963-3967.
- Q. Y. Zhang, Z. Fang, Y. Cao, H. M. Du, H. Wu, R. Beuerman, M. B. Chan-Park, H. W. Duan and R. Xu, *ACS Macro Lett.*, 2012, **1**, 876-881.
- G. S. Liou, P. H. Lin, H. J. Yen, Y. Y. Yu, T. W. Tsai and W. C. Chen, *J. Mater. Chem.*, 2010, **20**, 531-536.
- B. T. Liu, P. S. Li, W. C. Chen and Y. Y. Yu, *Eur. Polym. J.*, 2014, **50**, 54-60.
- L. H. Lee and W. C. Chen, *Chem. Mater.*, 2001, **13**, 1137-1142.
- J. G. Liu, Y. Nakamura, T. Ogura, Y. Shibasaki, S. Ando and M. Ueda, *Chem. Mater.*, 2008, **20**, 273-281.
- M. Sangermano, B. Voit, F. Sordo, K. J. Eichhorn and G. Rizza, *Polymer*, 2008, **49**, 2018-2022.
- S. Lee, H. J. Shin, S. M. Yoon, D. K. Yi, J. Y. Choi and U. Paik, *J. Mater. Chem.*, 2008, **18**, 1751-1755.
- G. Y. Zhang, H. Zhang, X. R. Zhang, S. J. Zhu, L. Zhang, Q. N. Meng, M. Y. Wang, Y. F. Li and B. Yang, *J. Mater. Chem.*, 2012, **22**, 21218-21224.
- F. Papadimitrakopoulos, P. Wisniecki and D. E. Bhagwagar, *Chem. Mater.*, 1997, **9**, 2928-2933.
- G. Y. Zhang, H. Zhang, H. T. Wei, S. J. Zhu, Z. N. Wu, Z. Y. Wang, F. Jia, J. B. Zhang and B. Yang, *Part. Part. Syst. Charact.*, 2013, **30**, 653-657.
- C. H. M. Chuang, P. R. Brown, V. Bulovic and M. G. Bawendi, *Nat. Mater.*, 2014, **13**, 796-801.
- A. Mihi, F. J. Beck, T. Lasanta, A. K. Rath and G. Konstantatos, *Adv. Mater.*, 2014, **26**, 443-448.
- A. R. Kirmani, G. H. Carey, M. Abdelsamie, B. Yan, D. Cha, L. R. Rollny, X. Cui, E. H. Sargent and A. Amassian, *Adv. Mater.*, 2014, **26**, 4717-4723.
- H. Althues, J. Henle and S. Kaskel, *Chem. Soc. Rev.*, 2007, **36**, 1454-1465.
- C. Lü and B. Yang, *J. Mater. Chem.*, 2009, **19**, 2884-2901.
- W. J. Bae, M. Trikeriotis, J. Sha, E. L. Schwartz, R. Rodriguez, P. Zimmerman, E. P. Giannelis and C. K. Ober, *J. Mater. Chem.*, 2010, **20**, 5186-5189.
- J. Fritsch, D. Mansfeld, M. Mehring, R. Wursche, J. Grothe and S. Kaskel, *Polymer*, 2011, **52**, 3263-3268.
- Y. Imai, A. Terahara, Y. Hakuta, K. Matsui, H. Hayashi and N. Ueno, *Eur. Polym. J.*, 2009, **45**, 630-638.
- J. M. Buriak, *Chem. Rev.*, 2002, **102**, 1271-1308.
- K. Jung, J. Y. Bae, S. J. Park, S. Yoo and B. S. Bae, *J. Mater. Chem.*, 2011, **21**, 1977-1983.
- Y. H. Kim, J. Y. Bae, J. Jin and B. S. Bae, *ACS Appl. Mater. Inter.*, 2014, **6**, 3115-3121.
- S. Sepeur, N. Kunze, B. Werner and H. Schmidt, *Thin Solid Films*, 1999, **351**, 216-219.
- Y. Yu, C. M. Hessel, T. D. Bogart, M. G. Panthani, M. R. Rasch and B. A. Korgel, *Langmuir*, 2013, **29**, 1533-1540.
- X. Cheng, R. Gondosiswanto, S. Ciampi, P. J. Reece and J. J. Gooding, *Chem. Commun.*, 2012, **48**, 11874-11876.
- J. J. Romero, M. J. Llansola-Portolés, M. L. Dell'Arciprete, H. B. Rodríguez, A. L. Moore and M. C. Gonzalez, *Chem. Mater.*, 2013, **25**, 3488-3498.
- X. Lu, C. M. Hessel, Y. Yu, T. D. Bogart and B. A. Korgel, *Nano Lett.*, 2013, **13**, 3101-3105.
- L. M. Wheeler, N. R. Neale, T. Chen and U. R. Kortshagen, *Nat. Commun.*, 2013, **4**, 2197.
- D. Mayeri, B. L. Phillips, M. P. Augustine and S. M. Kauzlarich, *Chem. Mater.*, 2001, **13**, 765-770.
- K. Seeger, *Semiconductor physics*, Springer-Verlag, 1982.